3rd URSI AT-AP-RASC, Gran Canaria, 29 May – 3 June 2022

A Hybrid Design Technique for Realizing Metasurface based Wideband and Wide Dual-Band Circularly Polarized Dielectric Resonator Antennas

Arslan Kiyani*(1), Nasimuddin Nasimuddin (2), Syed Muzahir Abbas (1,3), Mohsen Asadnia (1) and Karu P. Esselle(4)
(1) School of Engineering, Faculty of Science and Engineering, Macquarie University, Sydney, NSW, 2109, Australia
(2) Institute for Infocomm Research, Agency for science, Technology and Research (A*STAR), 138632, Singapore
(3) BENELEC, Botany, Sydney, NSW, 2019, Australia
(4) School of Electrical and Data Engineering, University of Technology Sydney (UTS), Sydney, NSW, 2007, Australia

Abstract

Compact, low-profile metasurface-based wideband and wide dual-band circularly polarized (CP) dielectric resonator antennas (DRAs) are presented in this paper. The rectangular-shaped DRs are loaded over two different types of strategic 7 × 7 metasurface unit cells including a "+" shape metasurface for single-band and square-slotted shape metasurface for dual-band performance. The DRs are fed diagonally with a single perturbed probe feed which is placed at an appropriate angle of 29°. Thus, the hybrid design combination of metasurface unit cells together with the angle of feed location from the center of DRs generates wideband CP radiation with enhanced 3-dB Axial Ratio (AR) and wide impedance matching bandwidths. Proposed antennas are successfully implemented and fabricated prototypes are measured demonstrating significant performance enhancement.

1. Introduction

With the rapid advances in wireless communication systems, the lightweight, compact and efficient antennas that offer high gain and wideband characteristics are highly demanded. Moreover, in order to integrate antennas with modern communication systems, polarization is considered one of the most prominent features [1]. Due to distinguished advantages such as feasible mobility, low cross talk, and improvement in multipath rejections, circularly polarized (CP) antennas are gaining significant precedence over linearly polarized antennas [2]. On the other hand, dielectric resonator antennas (DRA) are gaining an edge over microstrip antennas owing to their small size, high-quality factor, metallic lossless, no surface wave excitation, and higher radiation efficiency [3], [4].

DRAs demonstrating wide bandwidths were first presented in [5] and for circularly polarized radiation, several DRAs were proposed using a probe feed based on the perturbation method [6-7]. A maximum of 1.3% 3-dB axial ratio is demonstrated by these DRAs. Lately, to design compact antennas, the metasurface-based antennas are gaining substantial interest. Considerable designs have been proposed with an effort to integrate metasurface structures to antennas for improvement in performance [8], [9]. Since they offer the distinct capacity to manipulate the electromagnetic waves, the placement of metasurface either above or below the patch/radiators [10], [11], and recently on single layer led to realize wideband and high-gain operation. Furthermore, single feed CP microstrip antennas have been miniaturized using metasurface structures along with improvement in bandwidth [12], [13].

Nowadays realizing CP with dual and multi-bands is gaining more attraction. Researchers are trying to expand the system's capacity in order to support the growing user demands. Due to significant data applications, the available frequency resources are getting exhausted. Thus multi-band antennas hold apparent advantages as compared to single-band antennas. Considering this, various DRAs with dual-band operation are recently realized [14-17]. However, to the best of the author's knowledge, the proposed hybrid design technique is not exploited previously in the literature.

2. Wideband Circularly Polarized Dielectric Resonator Antenna

The design configuration of the proposed antenna is illustrated in Fig. 1. It comprises a single grounded substrate layer of FR4 (h_1 = 3.2 mm) and a rectangular DR made out of TMM10i dielectric substrate (h_2 = 6.5 mm, l = 14.9 mm, w = 12.6 mm) which is placed centrally over a 7 × 7 "+" shaped metasurface unit cell. The overall size of this FR4 substrate is 55 mm × 76 mm. Previously, standard square and rectangular-shaped metasurfaces are utilized by various researchers with the limitation of the narrow band. However, in this case, a plus-shaped metasurface unit cell is demonstrated to achieve a potential wideband response as shown in Fig. 2. It can be seen that the reflection phase bandwidth ranges from 4.9 GHz – 7 GHz depicting a broadband response. The normal and azimuth plane gaps between metasurface unit cells are 1.46 mm and 1.5 mm, respectively. These are fine-tuned to achieve the optimum performance. . The antenna structure is then excited with a single perturbed coaxial feed positioned at [x_o×cos(θ), x_o ×sin(θ)], x_o = 7.5 mm, θ = 29°] from the center of DR. The coaxial feed location is optimized along the diagonal line direction on the rectangular DR for a wideband CP radiation [18].

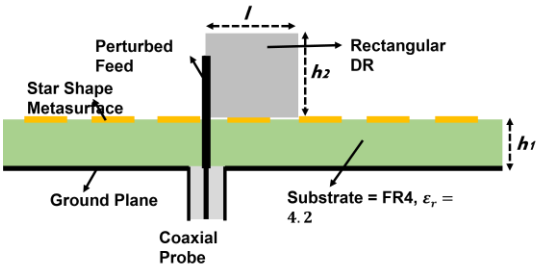

Figure 1. Cross-sectional view of the proposed antenna configuration

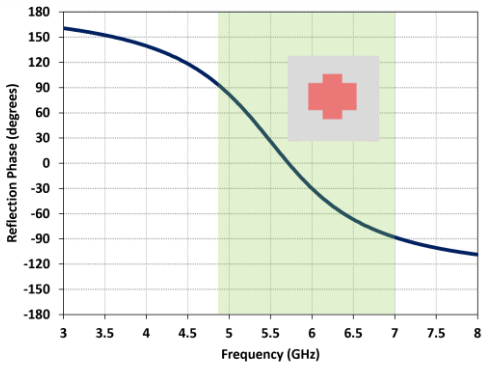

Figure 2. Reflection phase response of plus-shaped metasurface unit cell

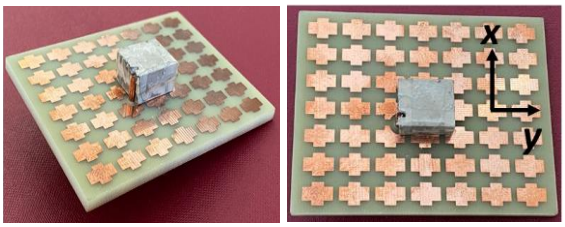

Figure 3. Fabricated antenna prototype

The prototype of the fabricated antenna is shown in Fig. 3 which is practically realized by using Agilent N5242A Vector Network Analyzer and NSI-700S-50 spherical near field chamber, available at the Australian Antenna Measurement Facility (AusAMF). DR is fixed over the metasurface using a thin adhesive tape and is fed using a standard 50-Ω probe feed connector. The comparison of predicted and measured input matching including $|S_{11}|$ and VSWR is presented in Fig 4 (a). The results can be seen in good agreement however, there is a slight shift in measured frequency. The measured second resonance is at 6.0 GHz as compared to the predicted second resonance at 5.65 GHz. This slight difference in the results is attributed due to the fabrication tolerances. It can either be due to the use of copper tape for realizing the perturbed probe feed or bit inconsistency while drilling the hole in the DR for excitation. The measured $|S_{11}|$ offers a wide impedance bandwidth of 32% ranging from 3.6 GHz to 7 GHz. Similarly, the measured 2:1-VSWR bandwidth ranges 34% from 3.4 GHz to 7 GHz, complementing a wide impedance matching within the operational frequency range.

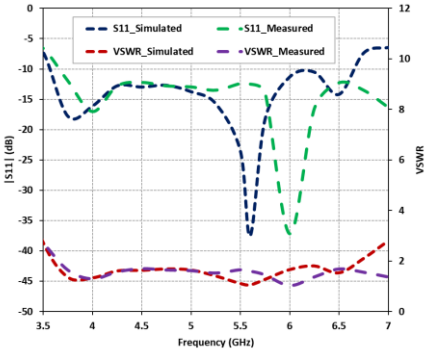

(a)

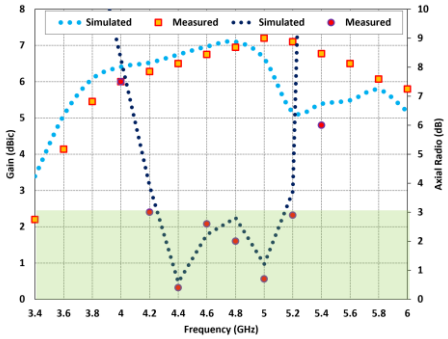

(b)

Figure 4. Comparison of predicted and measure antenna performance parameters (a) input matching ($|S_{11}|$, VSWR) (b) gain & AR

Fig. 4 (b) shows the antenna's predicted and measured gain and AR. In order to carry out the AR measurements, the 360° rotation method is used where a linearly transmitting antenna was fixed to measure the received signal from the proposed antenna. A wide 3-dB AR bandwidth of 20.4% ranging from 4.2 GHz to 5.2 GHz is achieved, with a 0.5 dB increment and a slightly shifted response as compared to the predicted 19% 3-dB AR bandwidth ranging from 4.45 GHz to 5.39 GHz. This might be due to the material tolerances or measurement errors resulting because of the rotating antenna alignment in the anechoic chamber. Moreover, from Fig. 4 (b), it can be observed that the measured gain range varies between 6-7 dBic across the operating frequency band.

3. Wide Dual-Band Circularly Polarized Dielectric Resonator Antenna

The design schematic of the proposed antenna is shown in Fig. 5. As compared to the wideband CP antenna presented in the previous section, this antenna is formed by stacking two rectangular DRs over a 7 × 7 square-slotted metasurface unit cell. First DR is made out of TMM3 dielectric substrate (h_2 = 1.524 mm, l_2 = 12.35 mm, w_2 = 22.23 mm) while second DR is made up of TMM3 dielectric substrate (h_3 = 1.524 mm, l_3 = 12.35 mm, w_3 = 22.23 mm). Both DRs are placed on top of a 45 mm × 65 mm FR4 (h_1 = 3.2 mm) grounded substrate and are excited with positioned coaxial feed [$x_o \times \cos(\theta)$, $x_o \times \sin(\theta)$], x_o = 7.43 mm, θ = 29°] along the diagonal line.

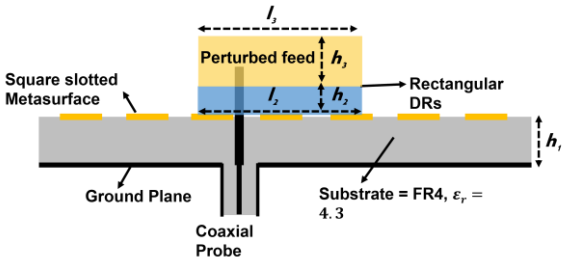

Figure 5. Schematic of the proposed antenna configuration

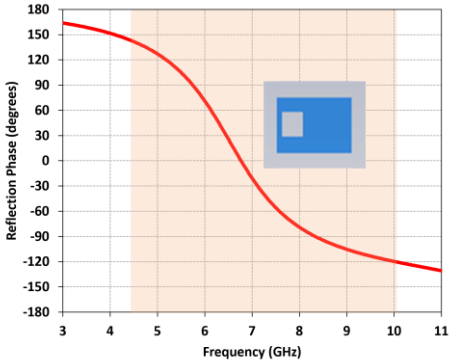

Figure 6. Reflection phase response of square-slotted shaped metasurface unit cell

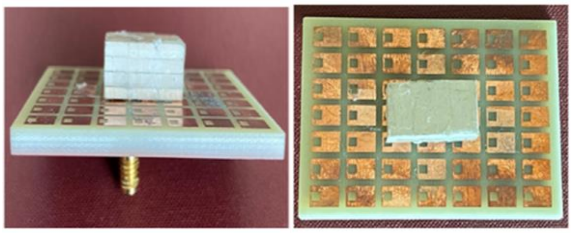

Figure 7. Fabricated antenna prototype

Fig. 6 shows the broadband reflection phase (±135°) of the square-slotted metasurface ranging from 4.6 GHz to 10.9 GHz. The normal and azimuth plane gaps between metasurface unit cells are 1.55 mm and 1.3 mm. The prototype of the fabricated antenna is shown in Fig. 7 and the measured results using Agilent N5242A Vector Network Analyzer and NSI-700S-50 spherical near field chamber are depicted in Fig. 8 (a) and 8 (b). From Fig. 8 (a), the measured results demonstrate that the predicted impedance bandwidth is 85.71% for $|S_{11}|$ from 4.0 GHz - 10 GHz and the measured impedance bandwidth is 88.1% for $|S_{11}|$ from 4.0 GHz - 10.3 GHz. Similarly, the predicted and measured VSWR bandwidth (VSWR$<$2) compliments the input matching ranging from (3.9 - $>$10 GHz). Fig. 8 (b) shows that the measured 3-dB AR bandwidths of lower and upper-frequency bands are 22.68% from 4.3 GHz to 5.4 GHz and 5.12% from 7.6 GHz to 8 GHz, respectively. This shows a good agreement between the predicted and measured AR plots at the boresight of the antenna. The measured gain values vary between 6 dBic to 8.4 dBic among lower and upper-frequency bands, with a peak measured gain of 8.4 dBic at 7.64 GHz.

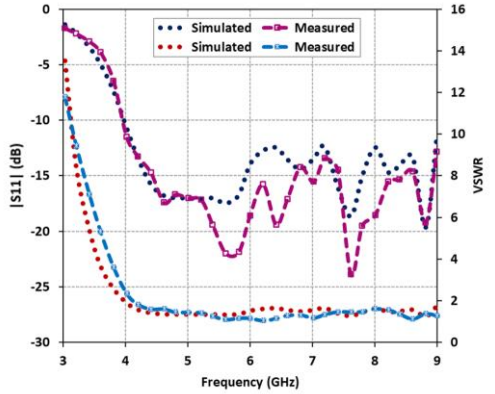

(a)

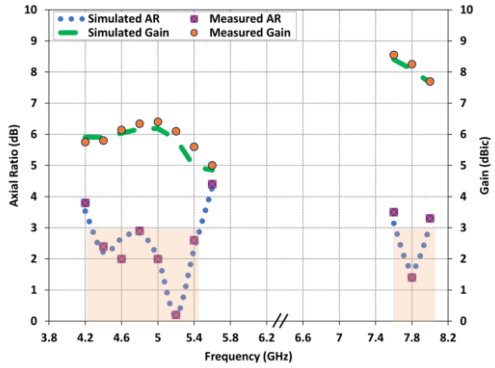

(b)

Figure 8. Comparison of predicted and measure antenna performance parameters (a) input matching ($|S_{11}|$, VSWR) (b) gain & AR

4. Conclusion

A hybrid design technique is demonstrated to realize thin metasurface-based DR antennas with wide single and dual-band CP operation. The antennas consist of rectangular DRs, strategic 7 × 7 metasurface unit cells, and a modified coaxial probe at a particular angle. Utilizing this feeding technique together with the well-matched metasurface unite cells, the radiation characteristics of both antennas including impedance bandwidth, axial ratio, and gain have been improved significantly. Overall, the proposed designs offer compact size, less complexity, and can be extended for application in multi-frequency band operation.

5. Acknowledgements

This work has been supported by the Australian Research Council and Macquarie University COVID Recovery Fellowship Scheme.

References

[1] Constantine A. Balanis: Antenna Theory: Analysis and Design, *Wiley & Sons*, **II** Edition, New York, 1997.

[2] S. Gao, Q. Lup, and F. Zhu: Circularly polarized antennas, *Wiley & Sons*, UK, 2014.

[3] A. Petosa: Dielectric Resonator Antenna Handbook, *Artech House*, **II** Edition, New York, 2007.
[4] K. P. Esselle, "A low-profile rectangular dielectric-resonator antenna," *IEEE Trans. Antennas Propag.*, **44**, 9, September 1996, pp. 1296-1297.
[5] Y. Ge, K. P. Esselle, and T. S. Bird, "Compact dielectric resonator antennas with ultra-wide 60%-110% bandwidths," *IEEE Trans. On Antennas and Propag.*, **59**, 9, September 1996, pp. 3445-3448.
[6] S. A. Malekabadi, M. H. Neshati, and J. Rashed-Mohassel, "Circular polarized dielectric resonator antennas using a single probe feed," *Progress in Electromagnetics Research C*, 3, 2008, pp. 81-94.
[7] P. Patel, B. Mukherjee, and J. Mukherjee, "Wideband circularly polarized rectangular dielectric resonator antennas using square-shaped slots," *IEEE Antennas and Wireless Propag. Lett.*, **15**, 2016, pp. 1309-1312.
[8] K. Agarwal, Nasimuddin, and A. Alphones, "RIS based compact circularly polarized microstrip antennas," *IEEE Antennas and Propag. Mag.*, **58**, 2, April 2016, pp. 39-46.
[9] N. Nasimuddin, Z. N. Chen and X. Qing, "Bandwidth enhancement of a single-feed circularly polarized antenna using a metasurface: metamaterial-based wideband CP rectangular microstrip antenna," *IEEE Trans. On Antennas and Propag.*, **59**, 9, September 1996, pp. 3445-3448.
[10] M. Faenzi, G. Minatti, D. Gonz´alez-Ovejero, F. Caminita, E. Martini, C. Della Giovampaola, and S. Maci, "Metasurface antennas: New models, applications and realizations," *Sci. Rep.*, **9**, 1, December 2019, pp. 1-14.
[11] I. Park, "Application of metasurfaces in the design of performance enhanced low-profile antennas," *EPJ, Applied Metamat.*, 2018.
[12] J. A. Sheersha, N. Nasimuddin, and A. Alphones, "A high gain wideband circularly polarized antenna with asymmetric metasurface," *Int. J. RF Microw. Comput.-Aided Eng.*, **29**, 7, July 2019.
[13] N. Hussain, M. Jeong, A. Abbas, and N. Kim, "Metasurface-based single-layer wideband circularly polarized MIMO antennas for 5G millimeter-wave systems," *IEEE Access*, **8**, 9, 2020, pp. 130293-130304.
[14] S. Gotra, G. Varshney, R. S. Yaduvanshi, and V. S. Pandey, "Dualband circular polarisation generation technique with the miniaturisation of a rectangular dielectric resonator antenna," *IET Microw., Antennas Propag.*, **13**, 10, August 2019, pp. 1742-1748.
[15] X. Fang, K. W. Leung, and E. H. Lim, "Singly-fed dual-band circularly polarized dielectric resonator antenna," *IEEE Antennas Wireless Propag.*, **13**, 2014, pp. 995-998.
[16] G. Varshney, S. Gotra, V. S. Pandey, R. S. Yaduvanshi, "Inverted-Sigmoid Shaped Multiband Dielectric Resonator Antenna with Dual Band Circular Polarization," *IEEE Trans. Antennas Propag.*, **66**, 2018, pp. 2067-2072.
[17] D. Pathak, S. K. Sharma, and V. S. Kushwah, "Dual-band circularly polarized dielectric resonator antenna for wireless applications," *Int. J. RF Microw. Comput.-Aided Eng.*, **28**, 5, 2018, Art. no. e21257.
[18] A. Kiyani, Nasimuddin, and K. P. Esselle, "A wideband circularly polarized dielectric resonator antenna over a metasurface," *IEEE International Symposium on Antennas and Propag. & USNC/URSI National Radio Science Meeting*, Boston, MA, 2018, pp. 2085-2086.